

Vascularity of the early post-natal human distal femoral chondroepiphysis: Quantitative MRI analysis

Kenneth M Lin¹, Naomi E Gadinsky¹, Craig E Klinger^{1,2}, Laura J Kleeblad³, Kevin G Shea⁴, Jonathan P Dyke⁵, David L Helfet^{1,2}, Scott A Rodeo¹, Daniel W Green¹, and Lionel E Lazaro⁶

Abstract

Purpose: Injury to or abnormality of developing distal femoral chondroepiphysis blood supply has been implicated in osteochondritis dissecans development. Progressive decrease in epiphyseal cartilage blood supply occurs in normal development; however, based on animal studies, it is hypothesized that there is greater decrease in regions more prone to osteochondritis dissecans lesions. We aimed to quantify differential regional perfusion of the immature distal femoral chondroepiphysis. We hypothesized there is decreased perfusion in the lateral aspect of the medial femoral condyle, the classic osteochondritis dissecans lesion location.

Methods: Five fresh-frozen human cadaveric knees (0–6 months old) were utilized. The superficial femoral artery was cannulated proximally and contrast-enhanced magnetic resonance imaging performed using a previously reported protocol for quantifying osseous and soft tissue perfusion. Regions of interest were defined, and signal enhancement changes between pre- and post-contrast images, normalized to background muscle, were compared.

Results: When comparing average normalized post-contrast signal enhancement of whole condyles, as well as distal, posterior, and inner (toward the notch) aspects of the medial and lateral condyles, no significant perfusion differences between condyles were found. In the medial condyle, no significant perfusion difference was found between the medial and lateral aspects.

Conclusion: We quantified immature distal femoral chondroepiphysis regional vascularity in the early post-natal knee. In specimens aged 0–6 months, no distinct watershed region was detected. Despite possible limitations, given small sample size, as well as resolution of magnetic resonance imaging and analysis, our results suggest the hypothesized vascular abnormality predisposing osteochondritis dissecans either does not occur universally or occurs after this developmental age.

Keywords: Chondroepiphysis vascularity, distal femur, post-natal, quantitative MRI, osteochondritis dissecans, diagnosis, basic science

Introduction

Osteochondritis dissecans (OCD) is a condition characterized by focal osteonecrosis of subchondral bone followed by collapse and destabilization of the overlying articular cartilage, which may result in premature osteoarthritis.^{1,2} It is typically seen in skeletally immature patients, with the lateral aspect of the medial femoral condyle of the knee being the most common location, although lesions of the lateral condyle, trochlea, and patella are seen as well.³ It is a relatively common condition, with an incidence of up to 18 in 100,000.^{4,5} OCD lesions may lead to accelerated development of osteoarthritis in young patients.⁵ Although the surgical treatment of OCD is well researched, with

¹Hospital for Special Surgery/New York Presbyterian Hospital/Weill Cornell Medicine, New York, NY, USA

²Orthopaedic Trauma Service, Hospital for Special Surgery, New York, NY, USA

³Northwest Clinics, Alkmaar, The Netherlands

⁴Stanford University Medical Center, Stanford, CA, USA

⁵Citigroup Biomedical Imaging Center and Weill Cornell Medicine, New York, NY, USA

⁶Miami Orthopedic & Sports Medicine Institute, Baptist Health South Florida, Miami, FL, USA

Date received: 14 April 2021; accepted: 7 February 2022

Corresponding Author:

Craig E Klinger, Orthopaedic Trauma Service, Hospital for Special Surgery, 535 East 70th Street, New York, NY 10021, USA.
Email: klingerc@hss.edu



numerous treatment options for different types of lesions, the exact cause of OCD remains unclear. Many potential etiologies have been proposed, including genetic factors, endocrine disorders, repetitive microtrauma, and vascular compromise leading to local ischemia during development.⁶⁻⁹ By understanding the etiology of OCD, it may become possible to identify patients who may be at risk or prevent development of symptomatic lesions.

Vascular compromise likely plays some role in the development of OCD lesions. During skeletal maturation, epiphyseal growth cartilage is supplied by temporary blood vessels running through cartilage canals. This blood supply diminishes as canals fill with cartilage; if it is abnormally diminished to focal regions, it is possible to develop localized ischemic necrosis of surrounding chondrocytes.¹⁰ These areas of ischemic chondronecrosis can cause delays in endochondral ossification as the ossification border reaches the damaged chondroepiphysis, potentially leading to subsequent subchondral bone defects.^{9,10} While numerous animal studies have shown that cartilage canal damage plays a key role in the development of osteochondrosis,¹¹⁻¹⁴ there are fewer human studies in the literature. Olstad et al.¹⁰ demonstrated in developing human cadaveric specimens that cartilage canal blood supply failure and ischemic chondronecrosis is seen histologically at predilection sites for juvenile OCD lesions. Tóth et al.¹⁵ also recently demonstrated a possible vascular watershed region in the developing human chondroepiphysis.

The current literature on the vascular etiology of OCD is largely limited to the microscopic scale, focusing on the cellular level. While important advancements have been made in our understanding of the biology of OCD, characterization of the in situ disease process in human knees is lacking. By quantifying perfusion patterns in a defined age group, important spatial and chronological information regarding predilection sites for OCD can be gained. The purpose of this study is to quantitatively characterize the differential arterial contribution to various regions of the distal femoral chondroepiphysis in intact early post-natal cadaveric knees using quantitative contrast-enhanced magnetic resonance imaging (MRI). Improved fundamental understanding of the pathogenesis of OCD will help guide early diagnosis, prevention, and etiology-based treatment which may alter natural history rather than only treating sequelae of an already clinically significant OCD lesion.

Methods

Cadaveric specimens

Following research approval of our Institutional Review Board, five fresh frozen skeletally immature human cadaveric knees (age of 0–6 months, mean age 3.0 months) were used for this study. Specimens were received from AlloSource (Centennial, CO, USA). Knee specimen used

included 4 males and 1 female. Specimens were included if they had an intact knee joint, from mid-femur to mid-tibia. Exclusion criteria included a history of lower extremity trauma, vascular disease, or lower extremity surgery. No specimens were from anatomically matched pairs. Cause of death of the specimens was not known, and time from death to tissue harvest was unknown.

Specimen dissection and preparation

Specimen dissection and preparation was performed in our institution's Bioskills Education Laboratory, which is an American College of Surgeons accredited dissection laboratory within our institution. Prior to imaging, the superficial femoral artery was cannulated proximal to the knee joint, along the femoral stump with minimal dissection performed and cannulas were sutured in place, as described previously for studying vascularity of intraarticular structures in the developing knee.^{16,17} For the cannulation procedure, vessel cannulas were used (DLP 30000, Medtronic, Minneapolis, MN). Infusion of normal saline was performed via syringe and all major extravasating vessels distal to the knee joint were tied off with silk ties.

MRI acquisition

Imaging was completed using a 3.0 Tesla Excite HD GE MRI scanner (General Electric Healthcare, Milwaukee, WI). An 8-channel wrist coil was used for the pediatric knees due to the smaller specimen size. Images were obtained using a previously described protocol, including the use of an 8-channel wrist coil, which was used for similar research focused on quantifying arterial contributions, including intraarticular soft tissue and bony structures in the developing knee.¹⁶⁻²⁰ Gadolinium-diethylenetriamine pentaacetic acid (Gd-DTPA) was diluted with normal saline at a ratio of 3:1 to serve as MRI contrast solution. The contrast solution volume utilized for the neonatal specimens (5 mL) was selected according to a previously published protocol using quantitative MRI to assess arterial contribution in neonatal knees of similar age.^{17,20} High-resolution fat-suppressed three-dimensional gradient echo sequences were obtained both prior to and following contrast solution injection. Fat-suppressed MRI images were used for quantitative MRI assessment purposes in order to remove signal generated by bone marrow while enhancing Gd-DTPA image detail. MR images were acquired both pre- and post-contrast solution infusion at 2 mm slice thickness. Post-contrast MRI was performed at one single time point, 10 min following contrast infusion. Images were reconstructed to achieve a resolution of $0.4 \times 0.4 \times 1.0$ mm. Image acquisition parameters consisted of repetition and echo times of 18.6 and 5.3 ms, respectively, using a 35° flip angle.

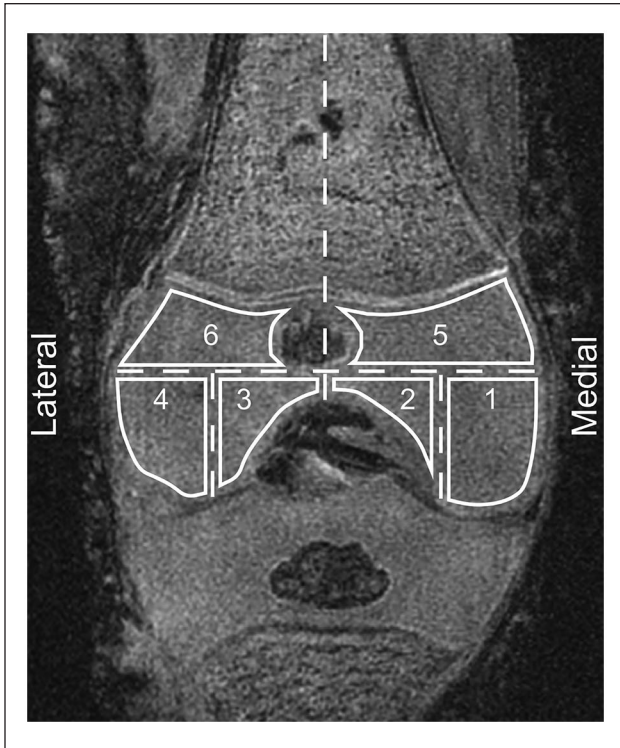


Figure 1. ROI zones used for quantification of post-contrast signal enhancement in the distal femoral chondroepiphysis.

Quantitative MRI analysis

For quantitative analysis, the distal femoral chondroepiphysis was divided into six regions of interest (ROI) zones distal to the growth plate excluding the secondary ossification center in each specimen (Figure 1). These ROIs were used to evaluate the increase in signal intensity from the defined ROI on the pre-contrast images to the same ROI area on the post-contrast images using software developed by a study investigator (J.P.D.) based on IDL 6.4 (Exelis, Boulder, Colorado).^{17,20} Signal enhancement was quantified to produce a weighted average, and raw signal intensity per voxel was corrected through normalization to nearby muscle as a baseline, as described previously.¹⁶ Increase in signal enhancement following contrast injection through the arterial system supplying the distal femoral chondroepiphysis was considered to represent arterial contribution.

Statistical analysis

Statistical analysis was performed using SPSS software (version 24, IBM). The increase in signal enhancement of the distal femoral chondroepiphysis is reported as the mean and standard deviation and as the median and interquartile range (IQR, 25%–75%). Data were not normally distributed, and therefore, Mann–Whitney U tests were used to compare the quantitative MRI findings between

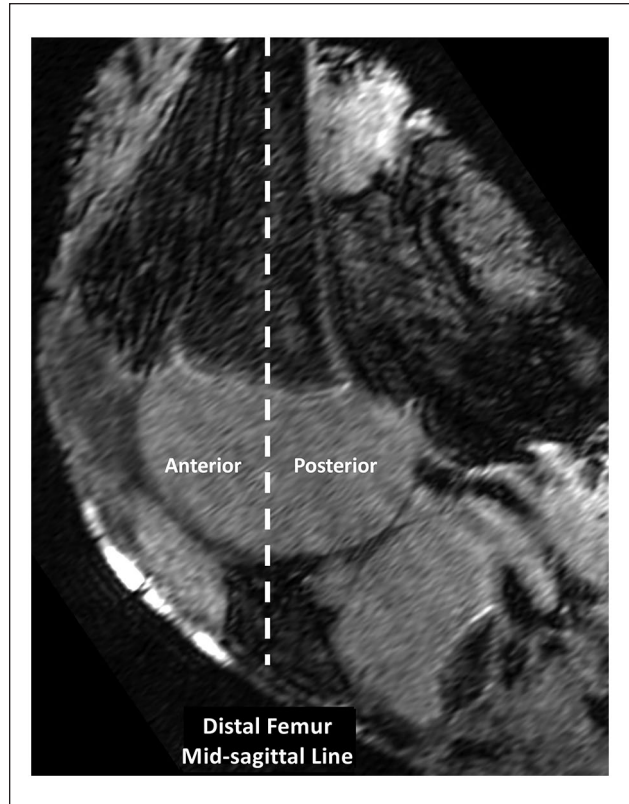


Figure 2. The medial and lateral condyles were divided into anterior and posterior sub-regions for quantification of post-contrast signal enhancement to the anterior and posterior aspects of the condyles. The mid-sagittal line was drawn on sagittal projections, and signal enhancement anterior or posterior to the sagittal midline was compared between medial (zones 1 and 2) and lateral (zones 3 and 4) condyles.

zones. Comparisons included medial versus lateral condyle (zones 1 + 2 + 5 versus 3 + 4 + 6), distal medial versus distal lateral condyle (zones 1 + 2 versus 3 + 4), posterior medial versus posterior lateral condyle (zones 1 + 2 posterior to the mid-sagittal line only versus zones 3 + 4 posterior to the mid-sagittal line only; Figure 2), inner medial versus inner lateral condyle (zone 2 versus 3), and medial versus lateral half of the medial condyle (zone 1 versus 2).

Results

Individual data for the relative arterial contribution to the six ROI zones for each individual specimen are presented in Table 1. Differences in normalized signal enhancement following contrast administration (which represents perfusion) were observed among the six zones, below the statistically significant threshold. When comparing average normalized post-contrast signal enhancement of whole medial versus lateral condyles, distal medial versus distal lateral condyles, posterior medial and posterior lateral condyles, and inner

Table 1. Individual ROI percent increase in signal enhancement following contrast administration.

Specimen data			Individual ROI zones					
SID	Months	Gender	1	2	3	4	5	6
1	0	F	10.4%	21.9%	10.5%	12.0%	22.8%	22.5%
2	2	M	19.4%	14.3%	17.7%	19.9%	15.3%	13.5%
3	2	M	17.0%	9.3%	10.3%	23.8%	17.0%	22.6%
4	5	M	11.6%	15.4%	16.5%	21.2%	22.6%	12.7%
5	6	M	19.5%	17.2%	21.9%	11.3%	17.7%	12.4%
		Mean	15.6%	15.6%	15.4%	17.6%	19.1%	16.7%
		SD	4.3%	4.6%	5.0%	5.7%	3.4%	5.3%
		Median	17.0%	15.4%	16.5%	19.9%	11.7%	13.5%
		Range	11.0%–19.4% ^a	11.8%–19.6% ^a	10.4%–19.8% ^a	11.6%–22.5% ^a	16.1%–22.7% ^a	12.6%–22.5% ^a

ROI: regions of interest; SID: specimen identification (number); SD: standard deviation.

^aRanges are reported as interquartile ranges (25–75th percentile).

Table 2. Average arterial contribution to various regions of medial versus lateral condyle.

Region	ROI zones	Average difference in signal enhancement (M-L, \pm SD)	p-value ^a
Whole condyles	M: 1, 2, 5 L: 3, 4, 6	0.5% (\pm 4.8% M, \pm 4.8% L)	0.917
Anterior whole condyles ^b	M: 1, 2, 5 L: 3, 4, 6	-1.6% (\pm 5.0% M, \pm 7.1% L)	0.917
Posterior whole condyles ^c	M: 1, 2, 5 L: 3, 4, 6	2.1% (\pm 4.1% M, \pm 5.1% L)	0.175
Proximal	M: 5 L: 6	2.3% (\pm 3.4% M, \pm 5.3% L)	0.251
Distal	M: 1, 2 L: 3, 4	0.2% (\pm 4.5% M, \pm 7.1% L)	0.917
Inner	M: 2 L: 3	0.2% (\pm 4.6% M, \pm 5.0% L)	0.754
Outer	M: 1 L: 4	-2.1% (\pm 4.3% M, \pm 5.7% L)	0.251
Anterior-distal ^b	M: 1, 2 L: 3, 4	-0.7 (\pm 3.2% M, \pm 3.5% L)	0.917
Posterior-distal ^c	M: 1, 2 L: 3, 4	-1.1% (\pm 2.6% M, \pm 6.1% L)	0.602

ROI: regions of interest; M: medial; L: lateral; SD: standard deviation.

^aMann–Whitney test.

^bAnterior to mid-sagittal line.

^cPosterior to mid-sagittal line.

aspects of the medial and lateral condyles, there was no significant difference in arterial contribution for any of the comparisons (Table 2). Within the medial condyle, the most common location for OCD lesions, no difference in arterial contribution between the inner (lateral) and outer (medial) aspects was observed in the early post-natal specimens (Figure 3).

Discussion

This study utilized qMRI to assess arterial contribution to various regions of the early post-natal human distal femoral chondroepiphysis. The results suggest nearly uniform

distribution of perfusion throughout the six designated ROI zones, without a distinct watershed region, in specimens aged 0–6 months. While a watershed area has been theorized to contribute to OCD lesions, it was not visible to qMRI in this study. The results may be interpreted to suggest that it may not be a universally occurring phenomenon, or may occur at a later point in life, and thus is not seen at the age of the study population. With only five specimens, this study may simply not have included any that would have gone on to have this phenomenon. Another consideration is that the theorized vascular insult is the result of the combined interaction of anatomic or genetic predisposing factor(s) with a traumatic insult to the

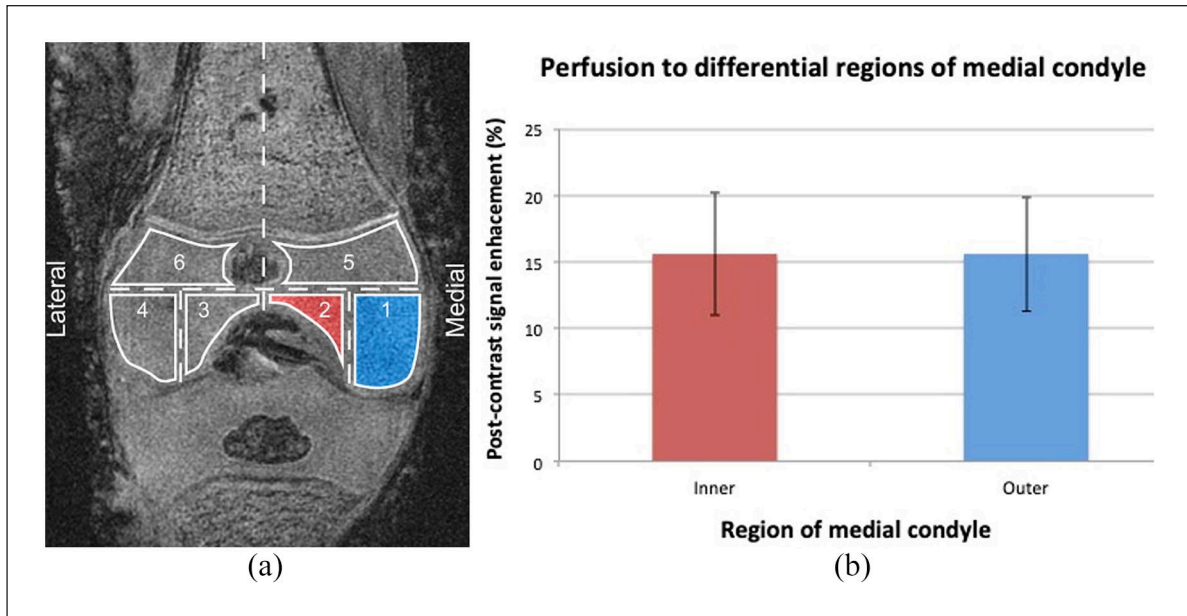


Figure 3. Perfusion to inner and outer aspects of the medial condyle: (a) schematic illustrates ROI zones used for quantification and (b) there was no difference in post-contrast signal enhancement to either side of the medial condyle (15.6% to both inner and outer regions); error bars represent standard deviation.

developing tissue; the phenotype may only be expressed if combined with a traumatic insult, more likely after the onset of weightbearing. Thus, the results of this study suggest that a watershed area is not a universal MRI-visible occurrence in the human knee from age 0 to 6 months. Improved fundamental understanding of the pathogenesis of OCD lesions will provide insight into improved treatment options.

In following with the developmental hypothesis for OCD, where and when the development of the OCD lesion departs from normal knee development is not yet known. Prior literature on vascular development of the human distal femoral chondroepiphysis is limited. Olstad et al.¹⁰ performed histologic analysis of 11 OCD lesions (from subjects age 7–11 years) identified by computed tomography scan, which showed that tissue from the lesions seen on imaging was consistent with ischemic chondronecrosis, suggesting a vascular etiology. Yousefzadeh et al.²¹ used grayscale and Doppler ultrasound to measure blood flow in cartilage of the human newborn and reported an age-related decline in the perfusion of the remaining unossified cartilage of the distal femur. Another study used gadolinium-enhanced MRI to image the normal epiphysis of children aged 1 month to 15.5 years and demonstrated that vascular cartilage canals decreased in number and changed their distribution with maturity.²² Jaramillo et al.²³ studied the proximal and distal femurs of 26 piglets aged 1–6 weeks old using contrast-enhanced MR images and found that with maturation, epiphyseal vascular canals became less noticeable and enhancement of the epiphyseal cartilage decreased. The findings of these studies reflect the normal

vascular changes occurring during maturation; as ossification progresses, the blood supply becomes increasingly concentrated in the ossification center, while the vascularity of the remaining epiphyseal cartilage declines.²¹ Tóth et al.¹⁵ utilized a susceptibility-weighted imaging (SWI) MRI sequence to examine the vascular architecture of the distal femoral epiphysis in three pigs and in five immature human cadaveric specimens ranging from 1 to 36 months old. In the human specimens, they found that the axial (central) vascular bed disappeared earlier in time than the vessels originating from the abaxial (peripheral) bed, leaving an avascular area near the inner region of the femoral condyles where OCD lesions often occur. While the current study also includes five human specimens, the age range is smaller and the vascularity gradient reported by Tóth et al. was not observed, suggesting that the vascular insult occurs at a later age in development. In the context of the prior literature, this study suggests that the vascular phenomenon in the developing chondroepiphysis that predispose to OCD lesions occurs after the early post-natal period. The study by Tóth et al.¹⁵ provides a complementary technique to visualize epiphyseal vasculature using a high-field 9.4T MRI without gadolinium. This technique could be used prior to administration of gadolinium to view the vasculature although a higher field strength magnet would need to be employed to get similar image resolution. Our technique evaluates tissue perfusion as the gadolinium leaks out of the vessels in comparison to SWI which does not provide extra-vascular information.

It is possible that the MRI technique used in this study may lack the sensitivity to detect a small vascular

abnormality in a smaller specimen (as the size of the distal femur changes markedly during early development and thus is much smaller in the specimens used in the current study). Prior studies using the current qMRI technique have detected differential vascularity gradients in the early post-natal meniscus and patella in knees of similar size, suggesting that differences in the distal femoral chondroepiphysis should be detectable. Given that MRI is a non-invasive imaging technique that is used in the clinical setting, this is an important pilot study that will allow us to use this protocol in specimens or patients at a more clinically relevant age. Use of older subjects would not only be a closer match to the ages used in prior studies but could also improve the sensitivity of the qMRI technique as the specimens being studied would be significantly larger in size. With an established protocol, this technique could potentially be used in live patients, although the possible side effects of gadolinium would need to be considered.^{24–26}

There are numerous important limitations to this study that must be considered in interpreting the findings. First, there is a small number of specimens given the scarcity of cadaveric tissue from young donors. This introduces sampling bias as the general population may not be represented in this limited number of study specimens. In addition, small sample size precludes a robust statistical analysis. However, the standard deviations reported in this study are quite small suggesting relatively little variability among the five study specimens from five separate donors (no matched pairs). Due to the rarity of specimens of this age group, there were no specimens of matching age with clinically evident OCD lesions. Second, although this study describes arterial contribution by perfusion techniques to the knee in situ (by way of cannulating the large vessels that supply the knee, without microscopic dissection, sectioning, and staining), it is a cadaveric study using contrast doses that may not be directly applicable to living subjects. It is known that large doses of gadolinium can be associated with toxicity in children.^{24,27} The age ranges studied are important for development of the knee, but are not directly clinically relevant, as patients would not present for evaluation at these ages. However, we studied the early post-natal age range as it is important to determine the time and location of a possible vascular insult to the distal femoral chondroepiphysis during development. Findings from this type of study are important for building an understanding of pathogenesis, which is integral for early diagnosis, possible prevention, and etiology-directed treatment strategies which may alter natural history, rather than treatment of the sequelae after an OCD lesion has already become clinically evident.

In summary, this study expands on our existing knowledge of the vascularity of the developing distal femoral chondroepiphysis. The results show uniform perfusion to

all areas of the early postnatal (0–6 months) developing chondroepiphysis, without a visible watershed region in the common predilection site for OCD lesions. The etiology of OCD remains poorly understood, as research in human subjects is limited due to ethical considerations in subjecting otherwise healthy children to invasive tests, and the difficulty in obtaining rare cadaveric specimens of relevant age. Improved fundamental understanding will help facilitate early diagnosis, prevention, and etiology-based treatment in the clinical setting.

Acknowledgements

The authors are grateful for funding for this study provided by the Hospital for Special Surgery Pediatric Service Research Award and also gratefully acknowledge AlloSource (Centennial, CO, USA) for providing the immature specimens utilized for this vascular research study.

Author contributions

K.M.L., N.E.G., C.E.K., and L.E.L. were involved in study design, data and MRI acquisition, MRI-ROI analysis, statistical analysis, preparation of the initial manuscript draft, and manuscript revisions. L.J.K. and J.P.D. were involved in study design, data and MRI acquisition, statistical analysis, preparation of the initial manuscript draft, and manuscript revisions. K.G.S., D.L.H., S.A.R., and D.W.G. were involved in study design, preparation of the initial manuscript draft, and manuscript revisions.

Declaration of conflicting interests

The author(s) declared the following potential conflicts of interest with respect to the research, authorship, and/or publication of this article: N.E.G., K.M.L., C.E.K., L.J.K., K.G.S., J.P.D., D.L.H., D.W.G., and L.E.L. declare that they have no conflict of interest. S.A.R. reports personal fees from Advance Medical/Teladoc, personal fees from Ortho RTI, Inc., outside the submitted work.

Funding

The author(s) disclosed receipt of the following financial support for the research, authorship, and/or publication of this article: This research was funded by an institutional research award from the Hospital for Special Surgery Pediatric Service Research Award, specifically the contrast-enhanced MRI imaging.

Compliance with ethical standards

This article does not contain any studies with human participants or animals performed by any of the authors and informed consent was not required. An Institutional Review Board exemption was provided for this cadaveric tissue study.

References

1. Hevesi M, Sanders TL, Pareek A, et al. Osteochondritis dissecans in the knee of skeletally immature patients: rates of persistent pain, osteoarthritis, and arthroplasty at mean 14-years' follow-up. *Cartilage* 2020; 11(3): 291–299.

2. Edmonds EW, Shea KG. Osteochondritis dissecans: editorial comment. *Clin Orthop Relat Res* 2013; 471(4): 1105–1106.
3. Kumar V, Bhatnagar N, Lodhi JS. Grade I osteochondritis dissecans in a young professional athlete. *Indian J Orthop* 2018; 52(4): 344–352.
4. Kessler JI, Nikizad H, Shea KG, et al. The demographics and epidemiology of osteochondritis dissecans of the knee in children and adolescents. *Am J Sports Med* 2014; 42(2): 320–326.
5. Nepple JJ, Milewski MD, Shea KG. Research in osteochondritis dissecans of the knee: 2016 update. *J Knee Surg* 2016; 29(7): 533–538.
6. Andriolo L, Crawford DC, Reale D, et al. Osteochondritis dissecans of the knee: etiology and pathogenetic mechanisms. A systematic review. *Cartilage* 2020; 11(3): 273–290.
7. Bauer KL. Osteochondral injuries of the knee in pediatric patients. *J Knee Surg* 2018; 31(5): 382–391.
8. Yellin JL, Trocle A, Grant SF, et al. Candidate loci are revealed by an initial genome-wide association study of juvenile osteochondritis dissecans. *J Pediatr Orthop* 2017; 37(1): e32–e36.
9. Ytrehus B, Carlson CS, Ekman S. Etiology and pathogenesis of osteochondrosis. *Vet Pathol* 2007; 44(4): 429–448.
10. Olstad K, Shea KG, Cannamela PC, et al. Juvenile osteochondritis dissecans of the knee is a result of failure of the blood supply to growth cartilage and osteochondrosis. *Osteoarthritis Cartilage* 2018; 26(12): 1691–1698.
11. Finnøy A, Olstad K, Lilledahl MB. Non-linear optical microscopy of cartilage canals in the distal femur of young pigs may reveal the cause of articular osteochondrosis. *BMC Vet Res* 2017; 13(1): 270.
12. Olstad K, Hendrickson EH, Carlson CS, et al. Transection of vessels in epiphyseal cartilage canals leads to osteochondrosis and osteochondrosis dissecans in the femoro-patellar joint of foals; a potential model of juvenile osteochondritis dissecans. *Osteoarthritis Cartilage* 2013; 21(5): 730–738.
13. Tóth F, Nissi MJ, Wang L, et al. Surgical induction, histological evaluation, and MRI identification of cartilage necrosis in the distal femur in goats to model early lesions of osteochondrosis. *Osteoarthritis Cartilage* 2015; 23(2): 300–307.
14. Tóth F, Nissi MJ, Zhang J, et al. Histological confirmation and biological significance of cartilage canals demonstrated using high field MRI in swine at predilection sites of osteochondrosis. *J Orthop Res* 2013; 31(12): 2006–2012.
15. Tóth F, Nissi MJ, Ellermann JM, et al. Novel application of magnetic resonance imaging demonstrates characteristic differences in vasculature at predilection sites of osteochondritis dissecans. *Am J Sports Med* 2015; 43(10): 2522–2527.
16. Lazaro LE, Wellman DS, Klinger CE, et al. Quantitative and qualitative assessment of bone perfusion and arterial contributions in a patellar fracture model using gadolinium-enhanced magnetic resonance imaging: a cadaveric study. *J Bone Joint Surg Am* 2013; 95(19): e1401–e1407.
17. Lin KM, Gadinsky NE, Klinger CE, et al. Increased vascularity in the neonatal versus adult meniscus: evaluation with magnetic resonance imaging. *Cartilage* 2021; 13: 1562S–1569S.
18. Dewar DC, Lazaro LE, Klinger CE, et al. The relative contribution of the medial and lateral femoral circumflex arteries to the vascularity of the head and neck of the femur: a quantitative MRI-based assessment. *Bone Joint J* 2016; 98-B(12): 1582–1588.
19. Boraiah S, Dyke JP, Hettrich C, et al. Assessment of vascularity of the femoral head using gadolinium (Gd-DTPA)-enhanced magnetic resonance imaging: a cadaver study. *J Bone Joint Surg Br* 2009; 91(1): 131–137.
20. Gadinsky NE, Lin KM, Klinger CE, et al. Quantitative assessment of the vascularity of the skeletally immature patella: a cadaveric study using MRI. *J Child Orthop* 2021; 15(2): 157–165.
21. Yousefzadeh DK, Doerger K, Sullivan C. The blood supply of early, late, and nonossifying cartilage: preliminary grayscale and Doppler assessment and their implications. *Pediatr Radiol* 2008; 38(2): 146–158.
22. Barnewolt CE, Shapiro F, Jaramillo D. Normal gadolinium-enhanced MR images of the developing appendicular skeleton: part I. Cartilaginous epiphysis and physis. *AJR Am J Roentgenol* 1997; 169(1): 183–189.
23. Jaramillo D, Villegas-Medina OL, Doty DK, et al. Age-related vascular changes in the epiphysis, physis, and metaphysis: normal findings on gadolinium-enhanced MRI of piglets. *AJR Am J Roentgenol* 2004; 182(2): 353–360.
24. Elbeshlawi I, AbdelBaki MS. Safety of gadolinium administration in children. *Pediatr Neurol* 2018; 86: 27–32.
25. Penfield JG. Nephrogenic systemic fibrosis and the use of gadolinium-based contrast agents. *Pediatr Nephrol* 2008; 23(12): 2121–2129.
26. Rozenfeld MN, Podberesky DJ. Gadolinium-based contrast agents in children. *Pediatr Radiol* 2018; 48(9): 1188–1196.
27. Pasquini L, Napolitano A, Visconti E, et al. Gadolinium-based contrast agent-related toxicities. *CNS Drugs* 2018; 32(3): 229–240.